Multi-layer Perceptron Diagnosis Method of Strip Surface Defects Based on Biogeography-Based Optimization Algorithm

Jia-Ning Hou, Jie-Sheng Wang*, Yu Liu

Abstract—**Detecting surface defects in strip steel is an essential step in the production process, and it has consistently held a prominent position in both domestic and international contexts. Stripping surface defects has a significant impact on the product's overall appearance. Moreover, it plays a crucial role in maintaining the strip product's wear resistance, corrosion resistance and fatigue strength. Failing to address these defects would inevitably result in a reduced service life for the strip product. This paper introduces a classification and diagnosis approach using the Multi-Layer Perceptron, optimized by the Biogeography-Based Optimization algorithm (BBO), for the purpose of diagnosing strip surface defects. The multi-layer perceptron is trained by using the BBO algorithm to find the best connection weight and bias value, so that it can identify the training set and test set, and make adjustments according to different needs. This paper carried out simulation experiments on strip surface defect data set in UCI data set. In this research, we evaluated the effectiveness of the proposed approach by benchmarking it against five alternative optimization algorithms. These included particle swarm optimization, ant colony optimization, distribution estimation algorithm, genetic algorithm, and extreme value search algorithm. It becomes evident that the accuracy and speed of the proposed method have experienced substantial enhancements. The application of the BBO algorithm in optimizing the multi-layer perceptron has been demonstrated to effectively address the challenge of diagnosing strip defects.**

Index Terms—**biogeography-based optimization algorithm, strip surface defect detection, multi-layer perceptron, migration model**

I. Introduction

The iron and steel industry has maintained a dominant position in the realm of economic development for a significant period. Within this industry, the strip product holds immense importance and finds extensive applications across various sectors of society. In the process of strip steel production, different types of defects will appear on the surface of the products due to various objective factors, such as, the raw materials used in the manufacturing process, rolling equipment and production technique. The types of strip surface defects can be broadly categorized as: pinholes, scars, scratches, abrasion, bonding, roll marks, holes, pitting and surface delamination [1]. These defects not only have a detrimental impact on the product's visual appeal, but also have the potential to diminish its overall performance. For example, they can result in a reduction in wear and corrosion resistance while concurrently enhancing fatigue strength. Consequently, the service life of the strip product is significantly compromised. Therefore, how to accurately detect the defects on the strip surface has become a concern of many colleges and universities at home and abroad and strip-related production enterprises. Finally, with the continuous efforts of researchers, a variety of detection methods came into being. In Ref. 2, the surface defects of steel strip are detected through the utilization of a classical convolutional neural network. However, this method has been enhanced by incorporating a transfer learning model. This alteration yields several benefits, such as shortened training time, accelerated convergence speed, and enhanced accuracy of weight parameters. In Ref. 3, an enhanced feature selection method is introduced, which combines a filtering method with a hidden Bayes classifier. Its goal is to enhance the efficiency of defect identification while simultaneously reducing computational complexity. This approach efficiently chooses the optimal mixed model, facilitating precise classification of surface defects in steel strips. Reference 4 introduced a stripe defect classification scheme that leverages ResNet50, along with the incorporation of FcaNet and the Convolutional Block Attention Module (CBAM). The integrated learning method was used to optimize the scheme, which improved the overall defect classification accuracy. In Reference 5, a novel deep neural network named the Depth Attention Residual Convolutional Neural Network is presented. This network has been tailored for the automatic detection of surface defects across six distinct categories of hot-rolled steel strips.

The inception of the Biogeography-based Optimization (BBO) algorithm dates back to 2008 when it was introduced by Professor Dan Simon. [6] and is then inspired by the principles of biogeography, which can be explained as a state of equilibrium in nature through species migration and drift between geographic regions. Here, the kind of information is among the determining variables of the optimization problem [7]. Much like other population-based optimization algorithms, the BBO algorithm also encompasses iterative processes involving species

Manuscript received June 17, 2023; revised October 8, 2023. This work was supported by the Basic Scientific Research Project of Institution of Higher Learning of Liaoning Province (Grant No. LJKZ0293), and Postgraduate Education Reform Project of Liaoning Province (Grant No. LNYJG2022137).

Jia-Ning Hou is a postgraduate student of School of Electronic and Information Engineering, University of Science and Technology Liaoning, Anshan, 114051, P. R. China (e-mail: 1994905806@qq.com).

Jie-Sheng Wang is a professor of School of Electronic and Information Engineering, University of Science and Technology Liaoning, Anshan, 114051, P. R. China (Corresponding author, phone: 86-0412-2538246; fax: 86-0412-2538244; e-mail: wang_jiesheng@126.com).

Yu Liu is an associate professor of School of Electronic and Information Engineering, University of Science and Technology Liaoning, Anshan, 114051, P. R. China (Ce-mail: lnasacl@126.com).

information, including migration and mutation operations. Within each generation, the individual exhibiting the highest fitness value is chosen as the global optimum .Ultimately, it identifies the optimal individual by means of population iteration and evaluation. In the BBO algorithm, the purpose of migration operations and exchange operations is to increase the diversity of species, thus contributing to global search, so it widely used by research scholars. Selvin proposed the chaotic BBO algorithm based on Selective Level Mapping (SLM) to provides an effective solution that exist in the orthogonal frequency division multiplexing waveform peak average power ratio problem [8]. Chen proposed a hybrid BBO algorithm to optimize the three-dimensional container size design and knapsack problems so as to maximize container volume utilization by optimizing the container size [9]. Reihanian introduced a pioneering evolutionary algorithm known as MOBCO-OCD, which incorporates a multi-objective Biogeography-based Optimization (BBO) approach. This algorithm is specifically tailored for the automatic identification of overlapping communities within social networks that incorporate node attributes. It considers both the network's connection density and the similarity of node attributes as crucial factors in the process [10]. Cao proposed the CCM-BBO framework, which utilizes the Cumulative Covariance Matrix (CCM) and has been proven to effectively obtain the global optimal values [11]. The Multi-layer Perceptron (MLP) proposed by Hinton was solved by the back-propagation algorithm [12] and the Sigmoid function was introduced in the propagation process between layers [13]. Introducing non-linearity to neural networks can improve the defect that single-layer perception cannot solve the XOR problem. The Multi-Layer Perceptron, abbreviated as MLP, is a feed-forward artificial neural network model that can effectively map multiple input datasets to a single output dataset [14], which has also been widely used in many practical applications. Elangovan has presented a feature selection based on classification algorithm for automated sentiment analysis by integrating Firefly algorithm and MLP technique [15]. Jamali provides a unique hyperspectral image classification method, based on complex MLP to solve the problems of high spatial dimension, huge number of spectral bands and few labeled data of hyperspectral images [16]. Wang introduced an approach based on Multi-Layer Perceptron (MLP) to discern commercial vehicle driving conditions. This method effectively addresses the challenge of classifying various commercial vehicle driving conditions, contributing to enhanced road traffic efficiency and sustainability. [17]

This paper presents a diagnostic method for strip surface defects based on the Biogeography-based Optimization (BBO) algorithm and Multi-Layer Perceptron (MLP). The paper is structured as follows: The second section outlines the training of the Multi-Layer Perceptron using the BBO algorithm. The third section covers experimental simulations and results analysis: The BBO algorithm is compared with five conventional intelligent algorithms, which include the Particle Swarm Optimization (PSO) algorithm [18], Ant Colony Optimization (ACO) algorithm [19], Genetic Algorithm (GA) [20], Population-Based Incremental Learning (PBIL) [21] and Extreme-value Search (ES) algorithm [22]. The steel plate defect data set is adopted in the simulation experiments under these six algorithms, the outcomes are then compared to validate the efficacy of utilizing the BBO algorithm for MLP neural network training. The final section presents the conclusion.

II. Biogeography-Based Optimization Algorithm

A. Overview of BBO Algorithm

Like other intelligent algorithms, the BBO algorithm falls under the category of population-based optimization methods. Nevertheless, it distinguishes itself by regarding each solution within the population as a habitat, with the solution's fitness level serving as the Habitat Suitability Index (HSI).Additionally, each component of the solution is considered a vector of Suitable Index Vector (SIV). The population evolves continuously by simulating the migration and mutation process in biogeography. When it comes to tackling optimization problems, the BBO algorithm exhibits distinctive characteristics that set it apart from other swarm intelligence optimization algorithms, including genetic algorithms, ant colony optimization algorithms, and particle swarm optimization algorithms. Firstly, it deviates from the conventional approach of reproduction or creation of the next generation. Secondly, Each generation solution is adjusted by migration probability. Finally, the biological incentive mechanism is adopted to select different operation intensity according to the population size of different habitats.

B. Mathematical Model of Biogeography

The following will introduce the species migration model of single HSI with migration rate μ and migration rate λ . A single species migration model on the island as shown in Fig. 1 was established, The graph depicts the relationship between the number of species on the X-axis and the corresponding probability on the Y-axis. It is clear that when the number of species is zero, the migration rate also reaches zero. However, as the number of species progressively increases, the space of the island becomes smaller, the number of species it can accommodate gradually reaches its peak, and the living conditions of the island will no longer be suitable. This kind of population then moves out to find a new habitat, resulting in a gradual increase in the migration rate. Once the maximum species capacity of the island reaches $S_{\max}$, the migration rate also reaches its maximum value E . Likewise, when the number of species reaches zero, the migration rate of the island reaches its peak value I . In the Fig.1, the population of species moving in and out reaches a balance at S_0 , $\mu = \lambda$, which means that the number of emigration is equal to that of emigration at this time, the population on the island enters a relatively stable state, and there will not be sudden large area migration or emigration.

Under normal circumstances, the migration model of species will be as complex as cosine curve and sine curve, and will not show a simple migration curve as shown in Fig. 1. Therefore, the process of migration in and out of the population will be described in details, and the migration model will be adjusted. In BBO algorithm, suppose that there are S species on an island, and its probability is P_s , which changes in time $[t, t+\Delta t]$ as follows:

$$P_s(t+\Delta t) = P_s(t)(1-\lambda_s\Delta t-\mu_s\Delta t)+ P_{s-1}\lambda_{s-1}\Delta t + P_s\mu_{s+1}\Delta t \quad (1)$$

When the number of species on the island reaches the number S, the move-in rate and migration rate of the island are μ_s and λ_s. Suppose the Eq. (1) holds, at $t+\Delta t$, there are S species. In this case, at least one of the following rule must be met:

(1) At t moment, there are S species on the island, and at the $[t,t+\Delta t]$, there are no species moving out and moving in.

(2) At t moment, there are $S+1$ species in the island, and at the $[t,t+\Delta t]$, one species migrates.

(3) At t moment, there are $S-1$ species on the island, and at the $[t,t+\Delta t]$, one species migrates.

When $\Delta t \to 0$, that is, Eq. (1) takes the limit and gives the variance show in Eq. (2). If define $n = S_{\max}$ and $P=[P_0,P_1,\cdots,P_n]^T$, $P_s(S=0,1,\cdots,n)$ is arranged into a single matrix.

$$P = AP \quad (2)$$

where, A is given in Eq. (4).

$$p=\begin{cases} -(\mu_s+\lambda_s)P_s+\mu_{s+1}P_{s+1}, S=0 \\ -(\mu_s+\lambda_s)P_s+\mu_{s-1}P_{s-1}+\mu_{s+1}P_{s+1}, 1\le S<S_{\max}-1 \\ -(\mu_s+\lambda_s)P_s+\mu_{s-1}P_{s-1}, S=S_{\max} \end{cases} \quad (3)$$

$$A=E\begin{bmatrix} -(\mu_0+\lambda_0) & \mu & 0 & \cdots & 0 \\ \lambda_0 & -(\mu_1+\lambda_1) & \mu_2 & \cdots & \cdots \\ \cdots & \cdots & \cdots & \cdots & \cdots \\ \cdots & \cdots & \lambda_{n-2} & -(\mu_{n-1}+\lambda_{n-1}) & \mu_n \\ 0 & \cdots & 0 & \lambda_{n-1} & -(\mu_n+\lambda_n) \end{bmatrix} \quad (4)$$

To facilitate the research, assume that $E=I$, Fig. (1) can be converted into Fig. 2.

$$\mu_k = \frac{E_k}{n} \quad (5)$$

$$\lambda_k = I\left(1-\frac{k}{n}\right) \quad (6)$$

where, $n=S_{\max}$ and k is the total number of species.

The probability of accommodating the number of species in each island can be defined as:

$$P_k=\begin{cases} P_0=\dfrac{1}{1+\sum_{l=1}^{n}\dfrac{\lambda_0\lambda_1\cdots\lambda_{l-1}}{\mu_1\mu_2\cdots\mu_l}}, k=0 \\ P_k=\dfrac{\lambda_0\lambda_1\cdots\lambda_{k-1}}{\mu_1\mu_2\cdots\mu_k\left(1+\sum_{l=1}^{n}\dfrac{\lambda_0\lambda_1\cdots\lambda_{l-1}}{\mu_1\mu_2\cdots\mu_l}\right)}, 1\le k\le n \end{cases} \quad (7)$$

If the species migration curves are the identical for each island (solution), then the result will be shown in Fig. 2, S_2 represents the high HSI solution and S_1 represents the low HSI solution. Through the analysis of each solution mobility, we share the information between the two islands. Six mathematical models of migration in BBO algorithm can be divided into linear and nonlinear, which are shown in Fig. 3.

C. Algorithm for Biogeography-Based Optimization

The BBO algorithm is composed of D-dimensional SIV with n habitats, where H_i represents the suitability of the i-th habitat, and all species with $S_{\max}$ value belong to H_i are extracted as n through the comparison of habitat H_i. Then the population S_i of the remaining habitats can be reduced one by one according to the order of H_i, that is, $S_i = S_{\max} - i$ ($i=1,2,\cdots,n$), where i is the arrangement of H_i according to their fitness. Through the calculation of the previous expression, we can get the rate of relocation μ and migration rate λ of i in the different migration model H_i. Thus the species accommodation probability $P(K_i)$ of H_i can be calculated by Eq. (8)..

$$M_S = M_{\max}.(1-\frac{P_S}{P_{\max}}) \quad (8)$$

Hence, the mutation rate M_i for each H_i is computed. The global variable is comprised of the maximum relocation rate E, the migration rate I, the $M_{\max}$ elite retention number $ZX_1,\ldots,X_n$ and the global mobility P_{mod}. The flowchart of the BBO algorithm is shown in Fig. 4. It can be seen from Fig. 4 that all the parameter variables of BBO algorithm are initialized firstly, then the suitability H_i of different habitats is arranged from good to bad, generally stipulating the habitat renewal rate $i=1$. By comparison, determine whether the result is the desired optimal. If yes, output the final optimum and end the optimization process. Otherwise, continue to get the species value S_i of habitat i through $S_i = S_{\max} - i$ ($i=1,2,\cdots,n$; $S_{\max}=n$), then bring it into the migration model to get the values of λ_i and μ_i. After a loop operation, it is determined whether it has entered the migration mode, and if i carries out the move-in operation, the SIV_{ij} of i can be replaced by the selected m component. Through the calculation of the M_i of the corresponding habitat, the algorithm assesses the pertinent habitat variables to identify any abrupt changes and then returns the comparison results for reuse.

D. BBO Algorithm to Optimize MLP Neural Network

(1) Multi-layer Perceptron (MLP)

Multi-layer perceptron (MLP) consists of an input layer, an output layer and a hidden layer. Within the MLP neural network, n represents the number of input nodes, h represents the number of hidden nodes, and m represents the number of output nodes.

The specific steps for calculating the output of MLP are as described as follows. Firstly, the weighted sum of the input is calculated by:

$$S_j = \sum_{i=1}^{n}\left(W_{ij},X_i\right)-\theta_j, j=1,2,\ldots,h \quad (9)$$

In this context, θ_j denotes the offset of the j-th hidden node, while X_i represents the i-th input node, with n denoting the total number of input nodes. Consider W_{ij} as the connection weight from the i-th node in the input layer to the i-th node in the hidden layer.

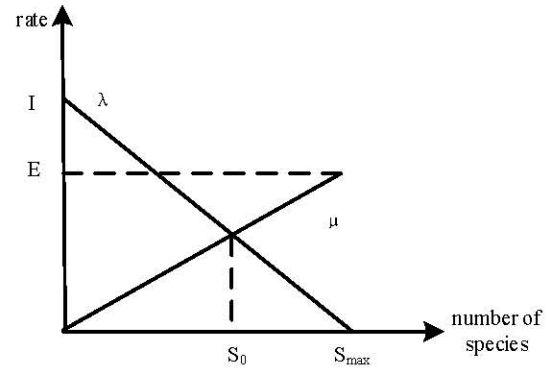

Fig. 1 A single island species migration model.

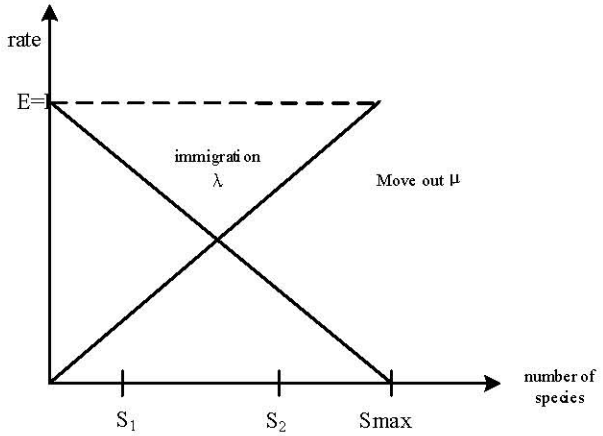

Fig. 2 Simplified species migration model based on a single island.

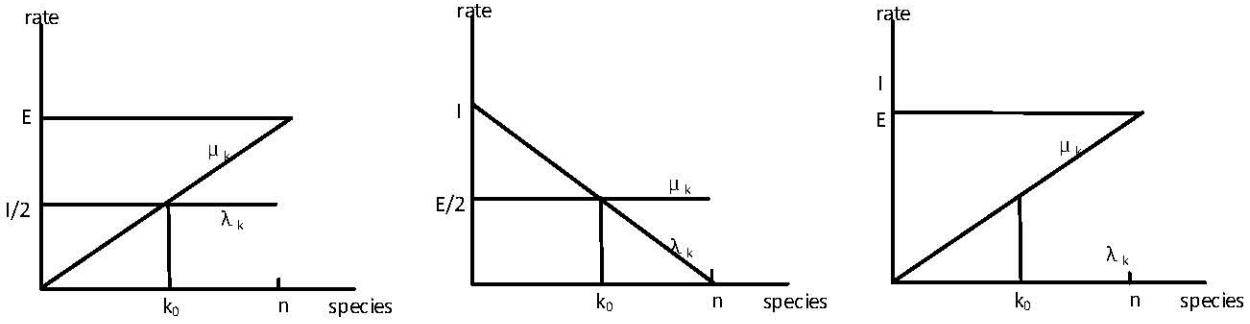

(a) Model 1 (b) Model 2 (c) Model 3

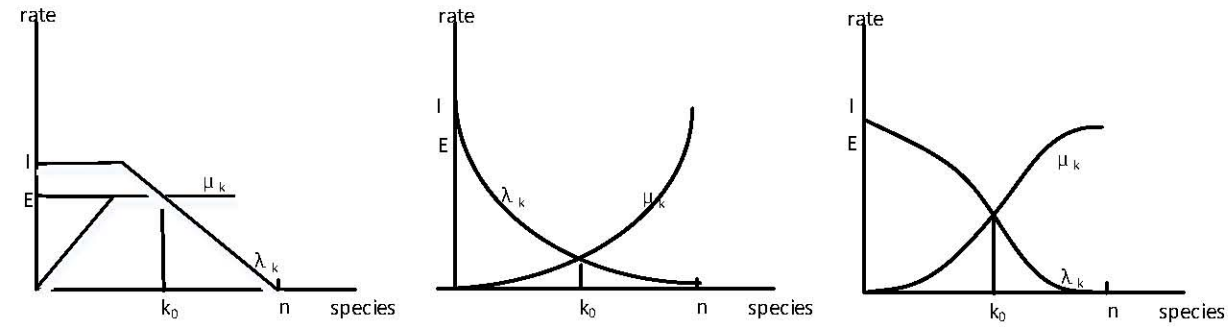

(d) Model 4 (e) Model 5 (f) Model 6

Fig. 3 Six models of BBO algorithm.

The computation for the output of each hidden node is described below:

$$O_k = sigmoid(O_k) = \frac{1}{1+\exp(-O_k)}, k = 1, 2, \ldots, m \quad (10)$$

The output of the hidden node is calculated by:

$$O_k = \sum_{j=1}^{h} (\omega_{jk}, S_j) - \theta'_k, k = 1, 2, \ldots, m \quad (11)$$

The final output is calculated by:

$$S_j = sigmoid(S_j) = \frac{1}{1+\exp(-S_j)}, j = 1, 2, \ldots, h \quad (12)$$

In this context, θ'_K represents the transpose of the k-th output node, while ω_{jk} represents the connection weight from the j-th hidden node to the k-th output node.

(2) Multi-layer Perception Optimized by BBO Algorithm

From the above formula, it can be seen that the connection weights and biases play a decisive role in the MLP neural network. From the above equation, it is not difficult to find that bias and weight affect the value of θ_k. A MLP neural network is trained so that it can better identify and capture training sets and test sets. In the whole process, the selection of training sets is also important. Each training sample should be applied to each habitat HSI calculation. In conclusion, the Mean Square Error (MSE) for all training samples is computed using Equation (13).

$$E = \sum_{k=1}^{q} \frac{\sum_{i=1}^{m} (o_i^k - d_i^k)^2}{q} \quad (13)$$

In this context, o_i^k denotes the actual output of the i-th input unit among the k training samples. q represents the total number of training samples, while d_i^k denotes the expected output of the i-th input unit within the k training samples. m represents the number of outputs. The

habitat suitability index (HSI) of the i -th habitat is calculated by using Eq. (14).

$$HSI\left(Habitat_i\right) = E\left(Habitat_i\right) \tag{14}$$

The process of training MLP is shown in Fig. 5.

III. Simulation Experiment and Result Analysis

A. Experimental Parameter Setting

The dataset for strip surface defects is sourced from the UCI database. This dataset comprises 1941 samples, and each sample contains 27 eigenvalues. Furthermore, the dataset includes seven distinct categories of steel plate defects, namely Pastry, Z_Scratch, K_Scratch, Stains, Dirtiness, Bumps, and Other_Faults. Table I offers representative examples of data from the strip surface subsidence dataset.

To evaluate the effectiveness of the proposed algorithm, this study undertakes a comparative analysis between the BBO algorithm and five conventional swarm intelligence algorithms, which include the Particle Swarm Optimization algorithm (PSO), Ant Colony Optimization algorithm (ACO), Genetic Algorithm (GA), Population-Based Incremental Learning (PBIL), and Extreme Search Algorithm (ES). The initialization of the parameters for each optimization algorithm is carried out. The habitat renewal probability, initial mutation probability, numerical integration step, maximum migration rate and migration rate of BBO algorithm are all 1. The pheromone update constant of ACO algorithm is 20. The parameter values are as follows: an exploration constant of 1, a global pheromone decay rate of 0.9, a local pheromone decay rate of 0.5, a pheromone sensitivity of 1, and a sensitivity of 5. The Genetic Algorithm (GA) utilizes a crossover probability of 0.85 and an initial mutation probability of 0.01. In the Population-Based Incremental Learning (PBIL) algorithm, the learning rate is set to 0.05, with both the probability vector mutation rate and the probability vector mutation rate set at 0. The Particle Swarm Optimization (PSO) algorithm employs an inertia constant of 0.3. Lastly, in the Extreme Search (ES) algorithm, each generation produces 10 offspring.

B. Multi-layer Perceptron Diagnosis Method of Strip Surface Defects Optimized by BBO Algorithm

To validate the effectiveness of the BBO algorithm adopted for training the MLP neural network to solve the strip surface defect identification problem, the ACO, PSO, GA, ES and PBIL algorithms are used to train MLP for carrying out the comparative experiments. 1240 data in the simulation experiment are used as the training dataset and 701 data as the verification dataset. To mitigate the influence of experiment randomness, 120 test samples are selected for each algorithm, and the experimental outcomes are illustrated in Figures 6 through 11. It can be seen that, except for the diagnosis on the first type of defects, the diagnosis effect of BBO-MLP algorithm for the other six types of defects tends to be stable and stable, and has been in the state closest to the expected effect compared with the other five algorithms. This also proves that the BBO-MLP algorithm is faster and more stable in the strip surface defect type diagnosis, and proves the effectiveness of the proposed algorithm.

As can be seen from Table II, the diagnosis accuracy of BBO algorithm for various types of defects is excellent among the six algorithms, and the overall accuracy is the highest of 85%, followed by GA and EA algorithms with an accuracy of 75%, ACO and PBIL algorithm with an accuracy of 70%. Among the six algorithms, PSO algorithm performs the worst, with an accuracy of 66.67%. The results show that BBO algorithm is the most effective in strip surface defect identification, GA and EA algorithms are the second, ACO and PBIL algorithms are slightly worse, and PSO algorithm is the least.

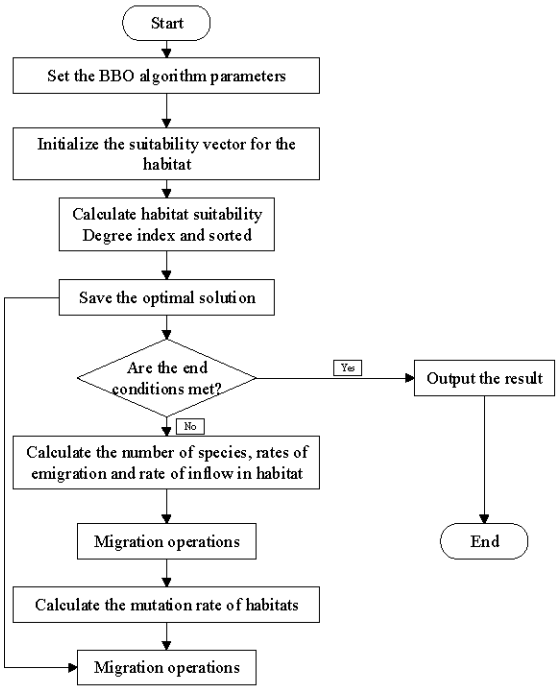

Fig. 4 Flow chart of BBO algorithm.

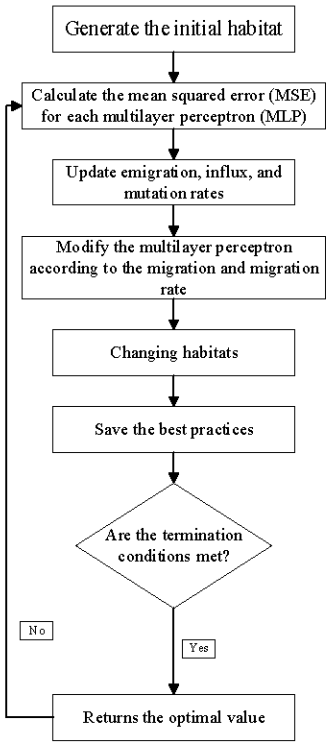

Fig. 5 Flow chart of BBO algorithm for training multi-layer perception.

TABLE I. DATASET OF STRIP SURFACE DEFECTS

Eigenvalue	Steel plate defects						
	Pastry	Z_Scratch	K_scratch	Stains	Dirtiness	Bumps	Other_Faults
X minima	42	1166	464	1002	1325	38	1108
X maximum	50	1185	4724	1027	1339	49	1120
Y minima	270900	2258648	28542	155255	30207	735612	2497122
Y maximum	270944	2258662	28553	155262	30238	735624	2497138
Pixel area	267	123	72	62	268	113	137
Perimeter of X	17	33	13	31	29	11	13
Perimeter of Y	44	17	12	9	31	12	16
Brightness combined	24220	15858	13094	7479	25809	12652	15672
Minimum brightness	76	116	168	114	79	93	85
Maximum brightness	108	143	198	132	124	130	133
Transport captain	1678	1708	1387	1360	1353	1707	1373
300 steel	1	1	0	1	0	1	0
400 steel	0	0	1	0	1	0	1
Plate thickness	80	100	40	100	120	100	40
Edge index	0.0498	0.6124	0.6691	0.4897	0.0207	0.0445	0.3685
Empty index	0.2415	0.5376	0.3455	0.6457	0.3825	0.1439	0.2845
Square index	0.1818	0.7368	0.9091	0.28	0.4516	0.9167	0.75
External index	0.0047	0.0111	0.0072	0.0184	0.0104	0.0064	0.0087
X edge index	0.4706	0.5758	0.7692	0.8065	0.4828	1	0.9231
Y edge index	1	0.8235	0.9167	0.7778	1	1	1
External index	1	0	1	0	1	1	1
Logarithmic area	2.4265	2.0899	1.8573	1.7924	2.4281	2.0531	2.1367
Logarithmic index	0.9031	1.2787	1	1.3979	1.1461	1.0414	1.0792
Logarithmic index	1.6435	1.1461	1.0414	0.8451	1.4914	1.0792	1.2041
Directional index	0.8182	-0.2632	0.0909	-0.72	0.5484	0.0833	0.25
Photometric index	-0.2913	0.0072	0.4208	-0.0576	-0.2476	-0.1253	-0.1063
B region	0.5822	0.4399	0.2173	0.2998	0.7065	0.2432	0.3241

This evidence further demonstrates that the BBO algorithm outperforms other typical intelligent optimization algorithms for the strip defects diagnosis, resulting in enhanced speed and accuracy compared to alternative algorithms. In addition, in the simulation process, firstly, the experimental verification results are based on the accuracy of each algorithm, but the results may change accordingly for different problems. Secondly, the parameters of the optimization algorithm are not deliberately adjusted, because the large changes in the performance of the optimization algorithm may be related to different parameter values, resulting in different conclusions. In summary, this experiment is intended to show that BBO algorithm is more advantageous in dealing with strip surface defect detection problems, compared with the traditional algorithm. It improves the speed and accuracy, and is very effective in dealing with conventional problems. Furthermore, this demonstrates that the Biogeography-Based Optimization algorithm, as a population-based approach, is effective in addressing engineering problems.

IV. CONCLUSIONS

This paper first analyzes the significance of strip surface defects in practice, describes strip steel, and studies the identification method of steel surface defects. In the second chapter, we delve into the design principles of the BBO algorithm, provide a detailed explanation of the algorithm flow for BBO optimization, present the training methodology for Multi-Layer Perceptron using the BBO algorithm, and introduce the associated training model. In the chapter of defect detection algorithm simulation experiment, six classical algorithms, namely BBO, GA, ES, ACO, PBIL and PSO, are introduced first, and their parameters are described. Subsequently, these algorithms are applied in conjunction with a strip defect dataset for conducting simulation experiments. The experimental outcomes demonstrate that the approach for strip surface defect detection, utilizing the BBO algorithm, exhibits substantial enhancements in terms of both accuracy and processing speed. Furthermore, the comparison with other optimization algorithms underscores the BBO algorithm's effectiveness and efficiency in addressing the challenge of strip defect diagnosis.

In this paper, the BBO algorithm is used to optimized the multi-layer perceptron diagnose model on strip surface defects. The adaptability of BBO algorithm exists in the process of biological habitat migration. The equilibrium price formation mechanism in the market regulation

mechanism is similar to the population migration mechanism in BBO algorithm. At the same time, this adaptive mechanism also plays an important role in many fields in the real world. BBO algorithm has reliable performance and obvious effect. The experimental results also show that it adopts the law formed by the long-term evolution of nature as the operating mechanism and is far superior to the typical intelligent optimization algorithms in dealing with strip surface identification problems.

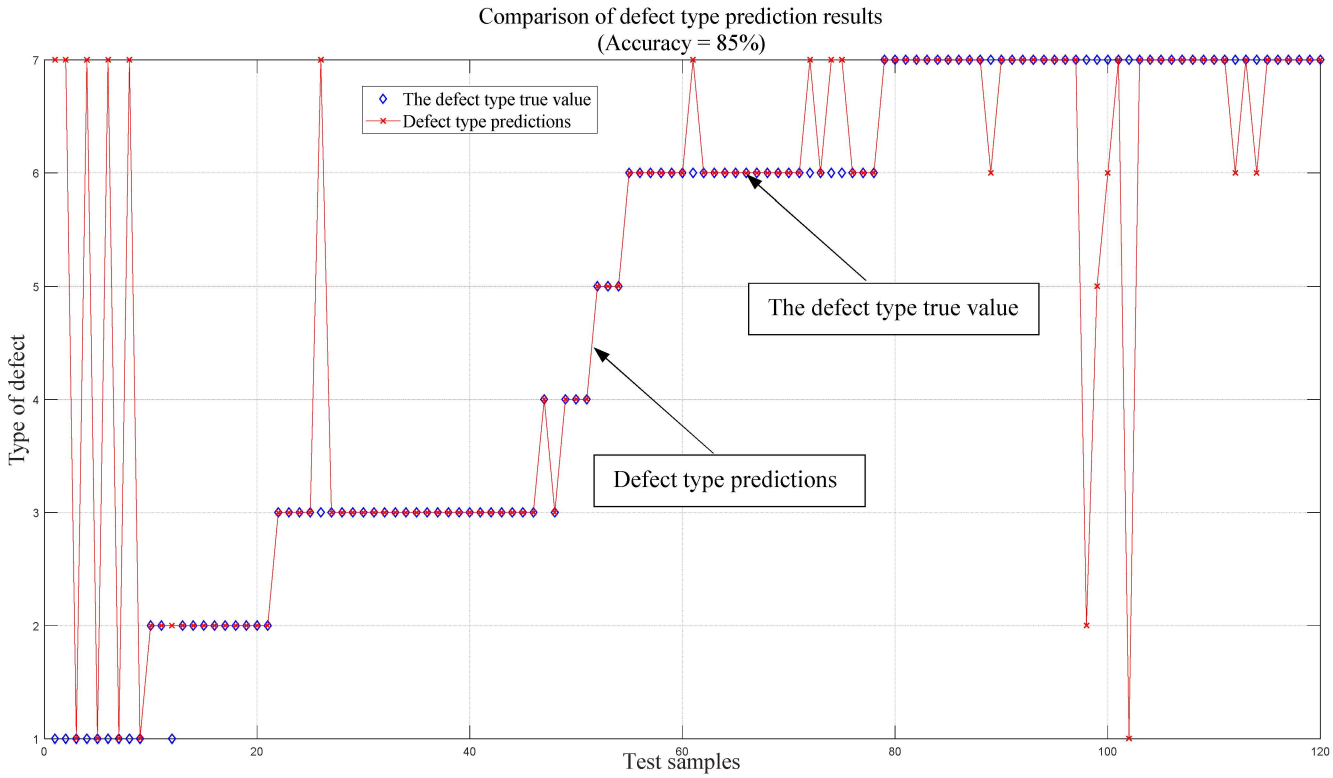

Fig. 6 Diagnose results of BBO-MLP algorithm.

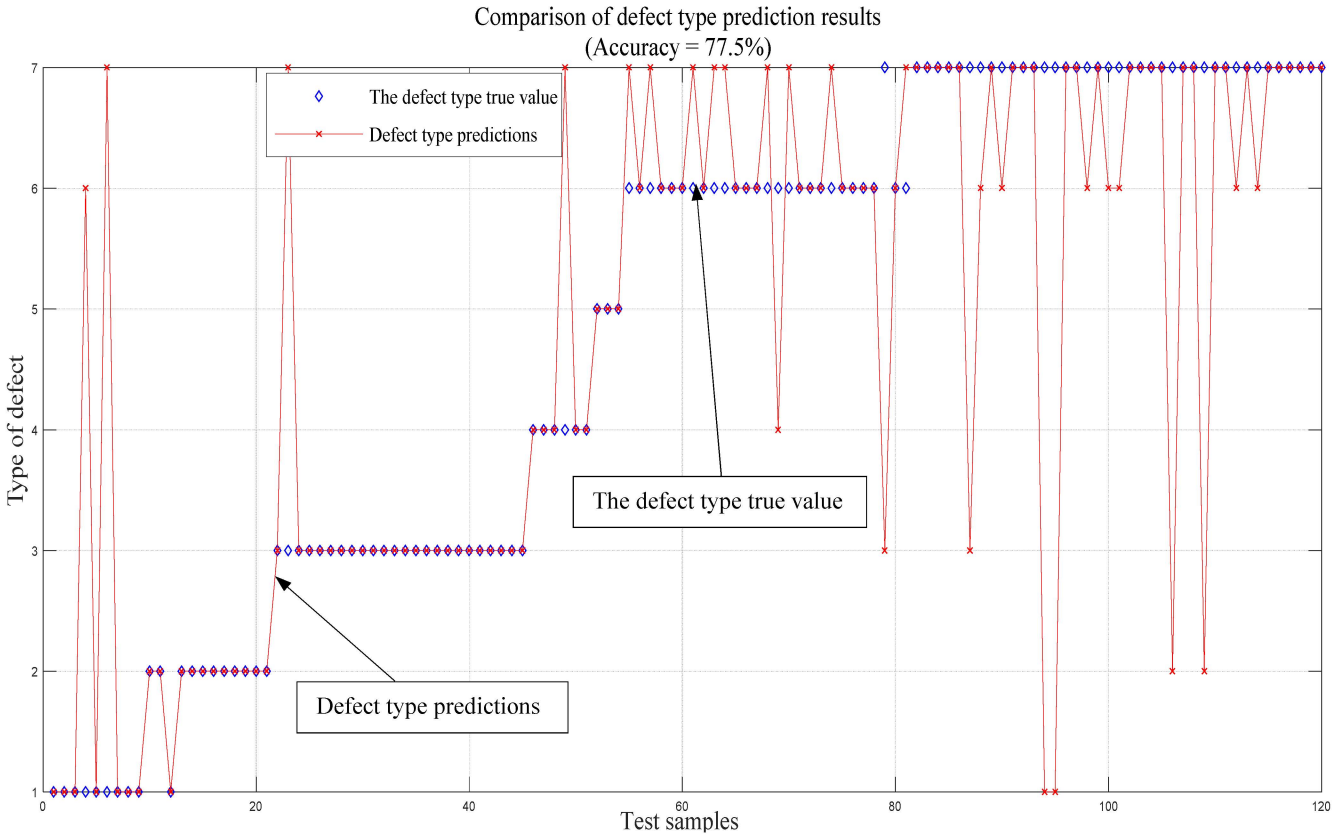

Fig. 7 Diagnose results of GA-MLP algorithm.

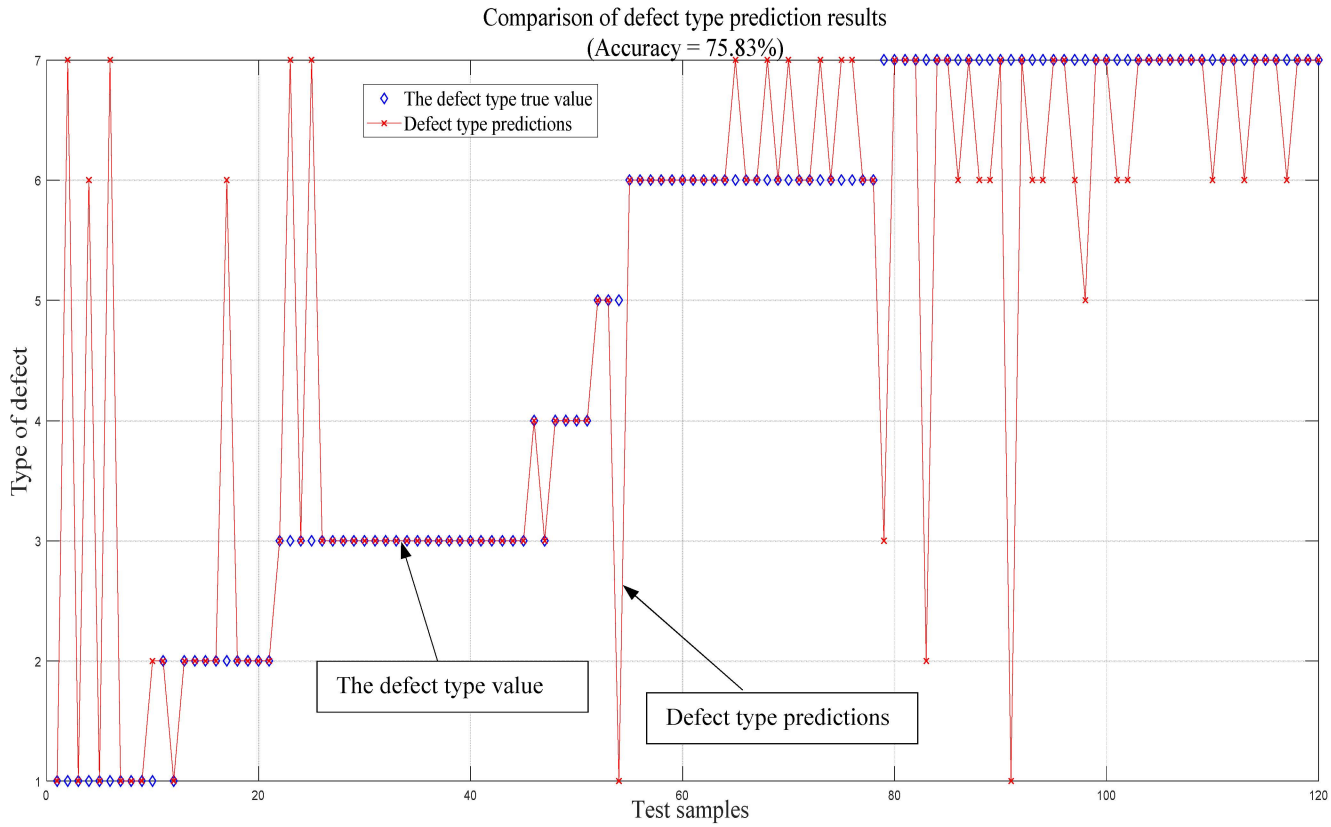

Fig. 8 Diagnose results of EA-MLP algorithm.

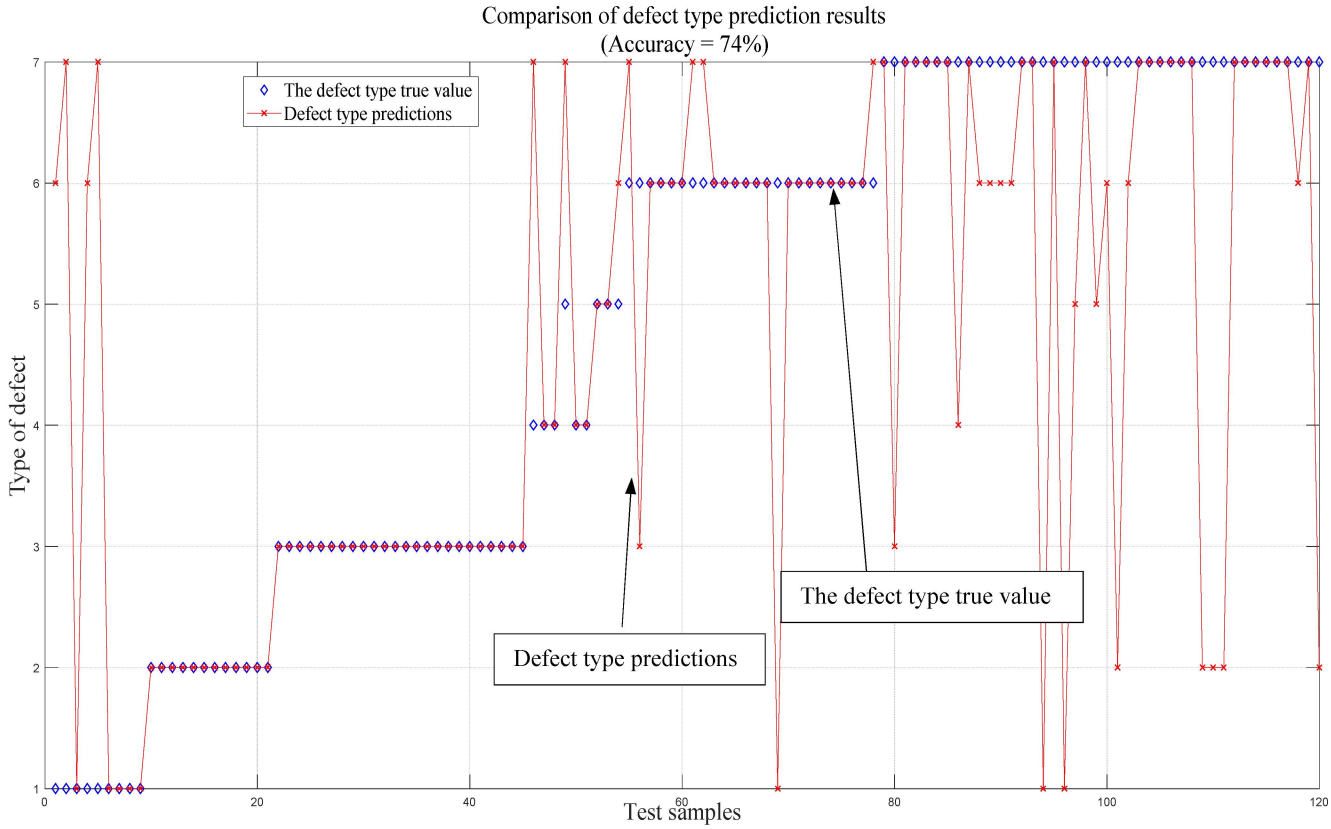

Fig. 9 Diagnose results of ACO-MLP algorithm.

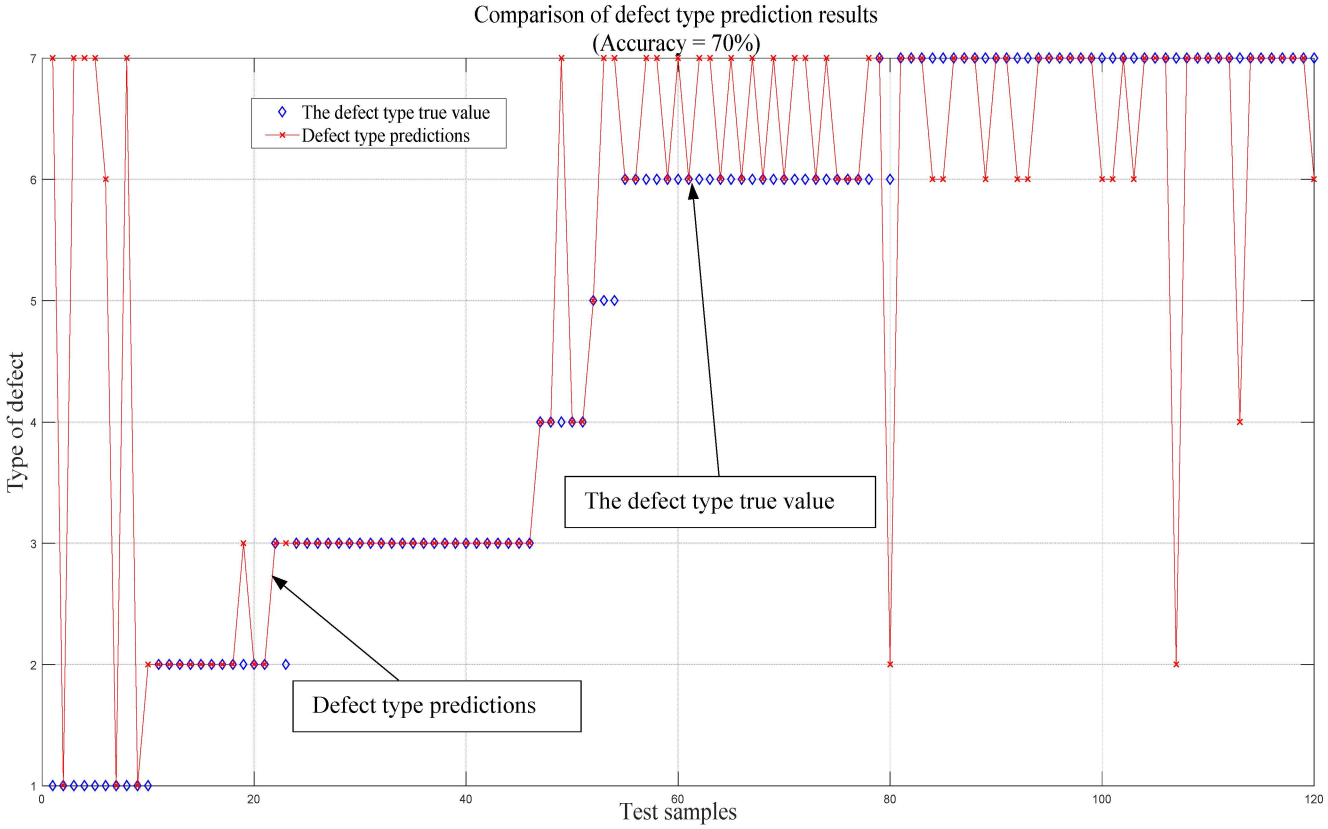

Fig. 10 Diagnose results of PBIL-MLP algorithm.

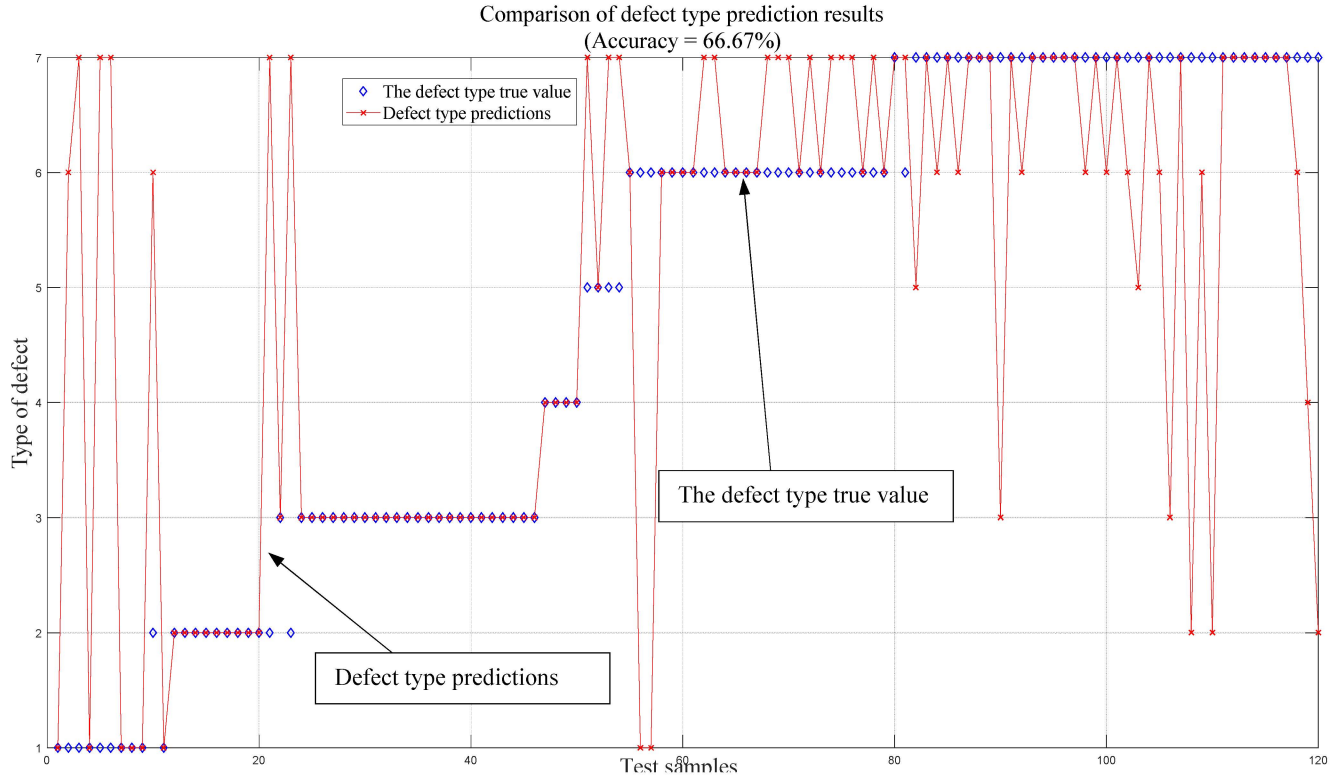

Fig. 11 Diagnose results of PSO-MLP algorithm.

TABLE II. DIAGNOSE RESULTS BASED ON DIFFERENT ALGORITHMS ON STRIP SURFACE DEFECTS

Strip surface defect	Diagnose methods					
	BBO-MLP	GA-MLP	EA-MLP	ACO-MLP	PBIL-MLP	PSO-MLP
Pastry	55%	78%	66%	56%	33%	54.54%
Z_Scratch	92%	90%	75%	100%	83%	90%
K_Scratch	96%	96%	92.6%	100%	96%	95.83%
Stains	80%	83%	83%	60%	80%	100%
Dirtiness	99%	70.5%	66.67%	67%	64%	25%
Bumps	83%	59%	71%	70%	55%	46.15%
Other_Faults	82%	66%	63.41%	65%	74%	56.41%
total	85%	77.5%	75.83%	74%	70%	66.67%

REFERENCES

[1] Z. X. Ma, Y. B. Li, M. H. Huang, and N. Z. Deng, "Online visual end-to-end detection monitoring on surface defect of aluminum strip under the industrial few-shot condition," *Journal of Manufacturing Systems*, vol. 70, no. 1, pp. 31-47, 2023.

[2] W. Hao, and Q.Q. Lv, "Hot-rolled steel strip surface inspection based on transfer learning model," *Journal of Sensors*, pp.1-8, 2021.

[3] Z. F. Zhang, W. Liu, E. Ostrosi, Y. J. Tian, and J. P. Yi, "Steel strip surface inspection through the combination of feature selection and multiclass classifiers," *Engineering Computations*, vol. 38, no. 4, pp. 1831-1850, 2021.

[4] X. Feng, X. Gao, and L. Luo,"A ResNet50-based method for classifying surface defects in hot-rolled strip steel," *Mathematics*, vol. 9, no.19, pp. 2359, 2021.

[5] Z. Huang, J. Wu, and F. Xie, "Automatic recognition of surface defects for hot-rolled steel strip based on deep attention residual convolutional neural network," *Materials Letters*, pp. 293, 2021.

[6] H. Moayedi, P. J. Canatalay, A. D. Ahmadi, and M. A. Cifci, "Multilayer perceptron and their comparison with two nature-inspired hybrid techniques of biogeography-based optimization (BBO) and backtracking search algorithm (BSA) for assessment of landslide susceptibility," *Land*, vol. 12, no. 1, pp. 242, 2023.

[7] J. D. Yao, K. O. Zemlianova, and D. L. Hocker, "Transformation of acoustic information to sensory decision variables in the parietal cortex," *Proceedings of the National Academy of Sciences*, vol. 120, no. 2, 2023.

[8] S. S. Kumar, K. C. Agees, R. R. Jemila, "An efficient SLM technique based on chaotic biogeography-based optimization algorithm for PAPR reduction in GFDM waveform," *Journal for Control, Measurement, Electronics, Computing and Communications,* vol. 64, no. 1, pp. 93-103, 2023.

[9] M. Chen, J. Huo, and Y. Duan, "A hybrid biogeography-based optimization algorithm for three-dimensional bin size designing and packing problem," *Computers & Industrial Engineering*, pp.180, 2023.

[10] A. Reihanian, M. R Feizi-Derakhshi, and H. S. Aghdasi, "An enhanced multi-objective biogeography-based optimization for overlapping community detection in social networks with node attributes," *Information Sciences*, vol. 622, pp. 903-929, 2023.

[11] Z. Cao, J. Li, and Y. Fu, "An adaptive biogeography-based optimization with cumulative covariance matrix for rule-based network intrusion detection," *Swarm and Evolutionary Computation*, pp. 75, 2022.

[12] N. Farouk, "Applying machine learning based on multilayer perceptron on building energy demand in presence of phase change material to drop cooling load," *Engineering Analysis with Boundary Elements*, vol. 150, pp. 20-29, 2023.

[13] R. Zhong, Y. Fu, and Y. Song, "A fusion approach to infrared and visible images with Gabor filter and sigmoid function," *Infrared Physics & Technology,* vol. 131, pp. 104696, 2023.

[14] H. Ye, Z. X. Liu, and Y. J. He, "Effects of M currents on the persistent activity of pyramidal neurons in mouse primary auditory cortex," *Journal of Neurophysiology*, vol. 127, no. 5, pp. 1269-1278, 2022.

[15] D. Elangovan, and V. Subedha, "Firefly with Levy based feature selection with multilayer perceptron for sentiment analysis," *Journal of Advances in Information Technology*, vol. 14, no. 2, 2023.

[16] A. Jamali, M. Mahdianpari, and R. A. Abdul, "Hyperspectral image classification using multi-layer perceptron mixer (MLP-MIXER)," *The International Archives of the Photogrammetry, Remote Sensing and Spatial Information Sciences*, vol. 48, pp. 179-182, 2023.

[17] X. Wang, Y. Zhao, and W. Li, "Recognition of commercial vehicle driving cycles based on multilayer perceptron model," *Sustainability,* vol. 15, no. 3, pp. 2644, 2023.

[18] D. Wang, D. Tan, and L. Liu, "Particle swarm optimization algorithm: an overview," *Soft computing*, vol. 22, pp. 387-408, 2018.

[19] M. Dorigo, M. Birattari, and T. Stutzle, "Ant colony optimization," *IEEE Computational Intelligence Magazine*, vol. 1, no. 4, pp. 28-39, 2006.

[20] S. Mirjalili, "Genetic algorithm," *Evolutionary Algorithms and Neural Networks: Theory and Applications*, pp. 43-55, 2019.

[21] S. Baluja, "Population-based incremental learning: A method for integrating genetic search based function optimization and competitive learning," *Pittsburgh, PA: School of Computer Science, Carnegie Mellon University*, 1994.

[22] L. F. Qian, Y. K. Ji, and Z. Y. Zhu, "Inverse estimation of wall temperature measurement under dispersion medium shielding based on CMA-ES algorithm," *Science and Technology for Energy Transition*, vol. 77, no. 16, 2022.